

A Magnetic Field Model for Wigglers and Undulators

D. Sagan, J. A. Crittenden, D. Rubin, E. Forest
Cornell University, Ithaca NY, USA
dcs16@cornell.edu

1. Analysis

One of the major challenges in designing the damping rings for the next generation of linear colliders is how to model the many wigglers that will be needed for emittance control. A prerequisite for the study of particle dynamics is the ability to calculate transfer maps. This is difficult for wigglers since analytic formulas do not exist except in the most simplified cases. Wigglers can have strong nonlinear components [1,2], which can be a major limitation on the dynamic aperture, and impose stringent conditions on any analytic approximations. Recently, a field model has been developed at Cornell that can be used to accurately track particles through a wiggler[3]. The advantages of the model are that it can be used to track symplectically and the model includes the end fields of the wiggler.

The field model is used with symplectic integration to do tracking. The symplectic integration algorithm was developed by Y. Yu et al [4]. The analysis starts with the Hamiltonian in the paraxial approximation

$$H = \frac{(p_x - a_x)^2}{2(1 + \Delta)} + \frac{(p_y - a_y)^2}{2(1 + \Delta)} - a_s,$$

where $p_{x,y} = P_{x,y}/P_0$ is the normalized transverse momentum, $\Delta = \Delta E/P_0 c$ is the relative energy deviation, z is the longitudinal position relative to the reference particle, and $\mathbf{a}(x,y,s) = q\mathbf{A}/P_0 c$ is the normalized vector potential. Yu has shown that by dividing this Hamiltonian in a certain way symplectic integration can be done. This procedure has been integrated into the PTC (Polymorphic Tracking Code) subroutine library of Etienne Forest [5] which in turn has been integrated into the Cornell BMAD particle simulation software library [6].

The BMAD library is written in Fortran90 and has been developed to supply a flexible framework that simplifies the task of writing custom programs to do particle simulations. The BMAD input format is very similar to the MAD input format so translating lattice files between the two formats is a fairly

simple task. Besides most of the standard MAD elements, BMAD recognizes wigglers, combination solenoid/quadrupoles, and LINAC accelerating cavities. Features include: Twiss parameter calculations, tracking, generating and manipulating Taylor Maps, Wakefields, etc.

2. Field Model

As input to the symplectic integrator one must have an analytical formula for the magnetic field that can be integrated to obtain the vector potential (the need to be able to repeatedly differentiate the vector potential precludes the alternative of interpolation from a field table). The Cornell wiggler field model starts by writing the field $B_{fit}(x, y, s)$ as a sum of terms

$$B_{fit} = \sum_{n=1}^N B_n(x, y, s; C_n, k_x, k_y, \varphi_n, f_n).$$

Each term B_n is parameterized by 5 quantities C , k_x , k_y , φ , and f . The index $f_n = 1, 2, \text{ or } 3$ is used to designate which of 3 forms a B_n term can take. The first form ($f_n = 1$) is

$$\begin{aligned} B_x &= C \frac{k_x}{k_y} \sin(k_x x) \sinh(k_y y) \cos(k_y s + \varphi) \\ B_y &= C \cos(k_x x) \cosh(k_y y) \cos(k_y s + \varphi) \\ B_s &= C \frac{k_y}{k_x} \cos(k_x x) \sinh(k_y y) \sin(k_y s + \varphi) \end{aligned} \quad (1)$$

with $k_y^2 = k_x^2 + k_s^2$

The second form ($f_n = 2$) is

$$\begin{aligned} B_x &= C \frac{k_x}{k_y} \sinh(k_x x) \sinh(k_y y) \cos(k_y s + \varphi) \\ B_y &= C \cosh(k_x x) \cosh(k_y y) \cos(k_y s + \varphi) \\ B_s &= C \frac{k_y}{k_x} \cosh(k_x x) \sinh(k_y y) \sin(k_y s + \varphi) \end{aligned} \quad (2)$$

with $k_y^2 = k_s^2 - k_x^2$

The third form ($f_n = 3$) is

$$\begin{aligned} B_x &= C \frac{k_x}{k_y} \sinh(k_x x) \sin(k_y y) \cos(k_y s + \varphi) \\ B_y &= C \cosh(k_x x) \cos(k_y y) \cos(k_y s + \varphi) \\ B_s &= C \frac{k_y}{k_x} \cosh(k_x x) \sin(k_y y) \sin(k_y s + \varphi) \end{aligned} \quad (3)$$

with $k_y^2 = k_x^2 - k_s^2$

k_y is considered to be a function of k_x and k_s . The relationship between them ensures that Maxwell's equations are satisfied.

Given a calculation or measurement of the field at a set of points \mathbf{B}_{data} , the problem is to find a set of N terms such that \mathbf{B}_{fit} and \mathbf{B}_{data} agree to some given precision set by how accurately one needs to be able to track through a wiggler. This is a standard problem in nonlinear optimization [7, 8]. The solution is to minimize a merit function M

$$M = \sum_{\text{data pts}} |B_{fit} - B_{data}|^2 + w_c \sum_{n=1}^N |C_n|$$

The second term in M is to help preclude solutions with degenerate terms that tend to cancel one another. The weight w_c should be set just large enough to prevent this but not so large as to unduly distort the fit.

3. CESR-c Wiggler Model

The wiggler magnets being installed in the Cornell CESR-c storage ring [9] have been modeled using the above procedure. Using the finite element modeling program OPERA-3D, a table of field versus position was generated. The validity of the field calculations was experimentally confirmed by measurements of tune as a function of beam position in a wiggler [10]. Table data and fit curves of B_y as a function of s and x for the CESR-c 8-pole wiggler are shown in Figures 1 and 2. 82 terms were used for the fit. The peak field is about 2 Tesla and the RMS of the difference $|\mathbf{B}_{data} - \mathbf{B}_{fit}|$ was 9 Gauss which gives an RMS to peak field ratio of 0.05%.

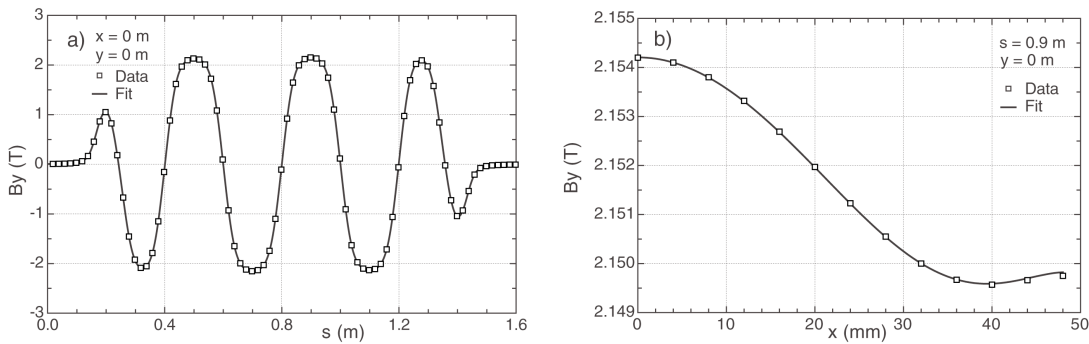


Figure 1: a) B_y as a function of s . b) B_y as a function of x . The data points are from a finite element modeling program. The curves are calculated from an 82 term fit.

Figures 2 and 3 show tracking simulation results for the CESR-c 8-pole wiggler. Figure 2 shows p_x at the end of the wiggler as a function of x at the start with a starting condition of $y = 20$ mm. Figure 3a shows p_y at the end as a function of y at the start with x_{start} set at 30 mm. The solid lines in Figures 2 and 3a are the results of using a Runge-Kutta (RK) integrator with adaptive step size control [7] and with the field values obtained from interpolating the table from OPERA-3D. The dashed lines are from symplectic integration (SI) using the fitted field and 250 integration steps. The dash-dotted lines are from a 7th order Taylor map (TM) which is generated using symplectic integration with 250 integration steps.

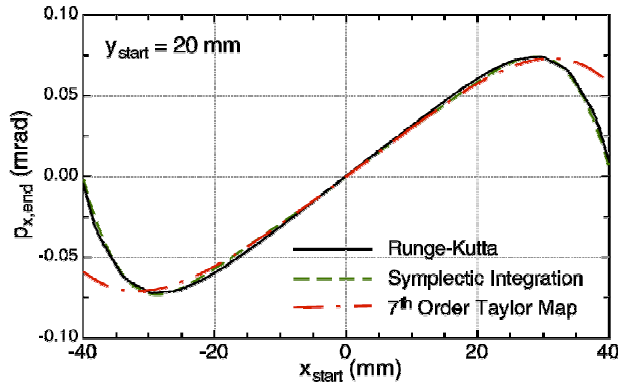


Figure 2: p_x at the end of the wiggler as a function of x at the start using 3 different tracking methods.

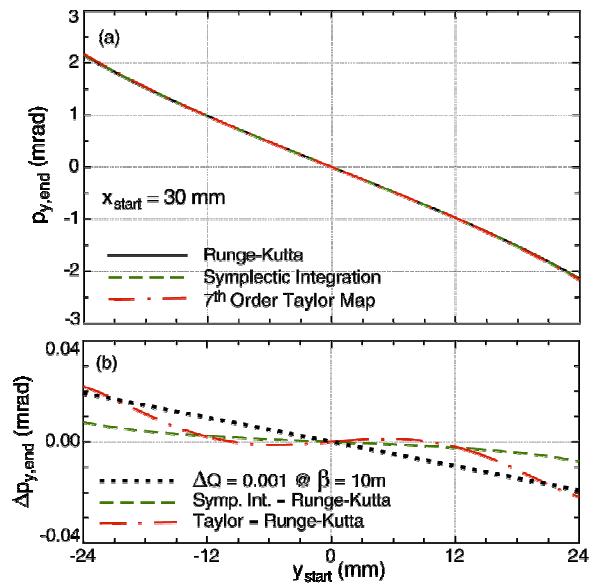


Figure 3: a) p_y at the end of the wiggler as a function of y at the start using 3 different tracking methods. b) Difference between RK tracking and the two other methods.

RK tracking, since it is derived directly from the equations of motion and the magnetic field table, is the gold standard with which to compare other tracking results. Figure 3b shows the difference between the SI and RK tracking as well as the difference between the TM and RK tracking. Additionally, for comparison, a line is shown whose slope represents a tune shift of $\Delta Q = 0.001$ assuming a β of 10 m. The SI tracking agrees well with the RK, better than 4 μ rad in Figures 2 and 8 μ rad in Figure 3. Slope differences of the curves are also small, representing tune shifts of less than

0.001 (at $\Delta = 10$ m) everywhere in the figures. The advantage of the SI tracking is that it preserves the Poincare invariants, such as phase space density, while the RK does not. This is an important consideration in long term tracking where RK can give unphysical results.

The TM also show excellent agreement with the RK tracking except in Figure 2 when the magnitude of x is larger than 30 mm or so. In the domain where the TM agrees with the RK, the TM can be used for such purposes as lattice design and other analyses that are not sensitive to non-symplectic errors. The advantage of the TM is that it is fast. In the present instance the TM was over a factor of 30 faster than the other two methods. (This does not include the time to calculate the TM to begin with, but that only has to be done once). To overcome the non-symplecticity of the TM it can be partially inverted to form a symplectic generating function [11].

4. Conclusion

The wiggler model is useful because it can accurately model a wiggler including end fields. This leads to efficient symplectic mapping which is needed in long term tracking, and avoids the non-physical violation of conserved quantities inherent when tracking is dependent upon interpolation of a field table. For applications where symplecticity is not a concern, a Taylor map, generated using the fit with symplectic integration can greatly reduce computation time.

For long periodic wigglers, the number of terms needed to fit the field may become large. In this case, a simple solution would be to divide the wiggler into 3 sections: the periodic center section and two end sections. Each section can be fitted separately. Since the center section is periodic, the number of terms needed to fit it is independent of its length. For the end sections it might be possible to cut down on the number of fit terms by making use of three additional forms that have an exponential s -dependence. These forms can be derived from (1), (2), and (3) using the substitution $k_s \rightarrow \Delta/k_s$.

If pole misalignments need to be simulated, then planar symmetry cannot be assumed. In this case, (1), (2), and (3) can be modified, at some small increase in complexity, by using $k_x x + \Delta_x$ in place of $k_x x$, and $k_y y + \Delta_y$ in place of $k_y y$. With this, any arbitrary magnetic field profile can be modeled.

References

1. P. Kuske, R. Gorgen, and J. Kuszynski, "Investigation of Non-Linear Beam Dynamics with Apple II-Type Undulators at Bessy II," Proc. 2001 Part. Acc. Conf., pg. 1656 (2001).
2. C. Milardi, D. Alesini, G. Benedetti, et al., "Effects of Nonlinear Terms in the Wiggler Magnets at DAΦNE," Proc. 2001 Part. Acc. Conf., pg. 1720 (2001).
3. D. Sagan, J. A. Crittenden, D. Rubin, "A Magnetic Field Model for Wigglers and Undulators," Proc. 2003 Part. Acc. Conf. (2003)
4. Y. Wu, E. Forest, D. S. Robin, H. Nishimura, A. Wolski, and V. N. Litvinenko, "Symplectic Models for General Insertion Devices," Proc. 2001 Part. Acc. Conf., pg. 398 (2001).
5. See: <http://bc1.lbl.gov/CBP_pages/educational/TPSA_DA/Introduction.html>.
6. D. Sagan, and D. Rubin, "CESR Lattice Design," Proc. 2001 Part. Acc. Conf., pg. 3517 (2001)
7. W. Press, B. Flannery, S. Teukolsky, and W. Wetterling, *Numerical Recipes in Fortran, the Art of Scientific Computing*, Second Edition, Cambridge University Press, New York, 1992.
8. F. James, *MINUIT, Function Minimization and Error Analysis*, CERN program library writeup D506.
9. J.A. Crittenden, A. Mikhailichenko, and A. Temnykh, "Design Considerations for the CESR-c Wiggler Magnets," Proc. 2003 Part. Acc. Conf. (2003).
10. A. Temnykh, J. A. Crittenden, D. Rice and D. Rubin, "Beam-based Characterization of a New 7-Pole Super-conducting Wiggler at CESR," Proc. 2003 Part. Acc. Conf. (2003).
11. E. Forest, *Beam Dynamics: A New Attitude and Framework*, Harwood Academic Publishers, Amsterdam (1998).